



ELSEVIER

Contents lists available at ScienceDirect

## Nuclear Instruments and Methods in Physics Research A

journal homepage: [www.elsevier.com/locate/nima](http://www.elsevier.com/locate/nima)

## Timing capabilities of garnet crystals for detection of high energy charged particles

M.T. Lucchini<sup>a,\*</sup>, S. Gundacker<sup>a</sup>, P. Lecoq<sup>a</sup>, A. Benaglia<sup>b</sup>, M. Nikl<sup>c</sup>, K. Kamada<sup>d,f</sup>,  
A. Yoshikawa<sup>d,e,f</sup>, E. Auffray<sup>a</sup><sup>a</sup> CERN, Geneva, Switzerland<sup>b</sup> Princeton University, Princeton, US<sup>c</sup> Institute of Physics AS CR, Prague, Czech Republic<sup>d</sup> Tohoku University, New Industry Creation Hatchery Center, Sendai, Japan<sup>e</sup> Tohoku University, Institute for Material Research, Sendai, Japan<sup>f</sup> C & A Corporation, T-Biz, Sendai, Japan

## ARTICLE INFO

## Keywords:

Precision timing  
Calorimeters  
Time-of-flight  
YAG:Ce  
LuAG:Ce  
GAGG:Ce  
LSO:Ce  
Crystals  
SiPM

## ABSTRACT

Particle detectors at future collider experiments will operate at high collision rates and thus will have to face high pile up and a harsh radiation environment. Precision timing capabilities can help in the reconstruction of physics events by mitigating pile up effects. In this context, radiation tolerant, scintillating crystals coupled to silicon photomultipliers (SiPMs) can provide a flexible and compact option for the implementation of a precision timing layer inside large particle detectors. In this paper, we compare the timing performance of aluminum garnet crystals (YAG: Ce, LuAG: Ce, GAGG: Ce) and the improvements of their time resolution by means of codoping with Mg<sup>2+</sup> ions. The crystals were read out using SiPMs from Hamamatsu glued to the rear end of the scintillator and their timing performance was evaluated by measuring the coincidence time resolution (CTR) of 150 GeV charged pions traversing a pair of crystals. The influence of crystal properties, such as density, light yield and decay kinetics on the timing performance is discussed.

The best single detector time resolutions are in the range of 23–30 ps (sigma) and only achieved by codoping the garnet crystals with divalent ions, such as Mg<sup>2+</sup>. The much faster scintillation decay in the co-doped samples as compared to non co-doped garnets explains the higher timing performance. Samples of LSO: Ce, Ca and LYSO:Ce crystals have also been used as reference time device and showed a time resolution at the level of 17 ps, in agreement with previous results.

## 1. Introduction

The capability to precisely measure the time of interaction of ionizing particles using radiation detectors is becoming a crucial aspect in medical imaging and high energy physics experiments. A detector with a time resolution at the level of tens of picoseconds would allow to improve image reconstruction in positron emission tomography (PET) scanners [1–4] and would permit to mitigate the effects of event pile up in high luminosity collider detectors, which operate under high rate conditions [5]. Previous studies demonstrated the capability to achieve sub-20 ps time resolution using devices consisting of L(Y)SO:Ce and LSO: Ce, Ca crystals read out with silicon photomultipliers (SiPM) [6]. In this context, LSO:Ce and LYSO:Ce crystals represent excellent candidates for timing applications due to their high light yield (40000 ph/MeV) and relatively fast decay time (40 ns). In addition, it

has been shown that Ca<sup>2+</sup> codoping improves the scintillation characteristics of Ce-doped LSO by suppression of slow delayed recombination processes with consequent decrease of the scintillation decay time down to 31 ns [7,8]. Similar and very encouraging studies have recently demonstrated the possibility to improve the scintillation properties of aluminum garnet crystals, such as YAG: Ce, LuAG:Ce and GAGG: Ce, by codoping with Ca<sup>2+</sup> and Mg<sup>2+</sup> ions [9–11]. The faster scintillation pulses achievable in such codoped crystals make them an attractive and promising option for timing applications. In particular, GAGG:Ce crystals show a light yield higher than LSO:Ce and good timing has already been measured for Mg-codoped samples using low energy  $\gamma$ -rays despite the slower scintillation time profile [4,12]. As aluminum garnet crystals have also been proven to be extremely radiation tolerant to high levels of ionizing radiation and hadron fluences they can operate in harsh radiation environments such as those of future hadron

\* Corresponding author.

E-mail address: [Marco.Toliman.Lucchini@cern.ch](mailto:Marco.Toliman.Lucchini@cern.ch) (M.T. Lucchini).<http://dx.doi.org/10.1016/j.nima.2017.02.008>

Received 6 December 2016; Received in revised form 30 January 2017; Accepted 3 February 2017

Available online 04 February 2017

0168-9002/ © 2017 CERN for the benefit of the Authors. Published by Elsevier B.V. This is an open access article under the CC BY license (<http://creativecommons.org/licenses/by/4.0/>).

colliders [13]. In this paper we investigate and discuss the improved timing capabilities of garnet crystals codoped with  $Mg^{2+}$  ions (YAG, LuAG, GAGG), for high energy physics applications. Timing results obtained with LYSO:Ce and LSO: Ce, Ca crystals used as reference time detectors are also discussed. An overview of the optical and scintillation properties of the crystals is also given and discussed in relation to the timing performance achieved for detection of 150 GeV pions.

## 2. Experimental methods

### 2.1. Crystal samples

Six different Ce-doped garnet crystals have been used for this test: one LuAG: Ce, one YAG: Ce, one GAGG:Ce and the corresponding samples codoped with  $Mg^{2+}$  ions (i.e. LuAG: Ce,Mg, YAG: Ce,Mg and GAGG: Ce,Mg). Two pairs of  $2 \times 2 \times 5 \text{ mm}^3$  and  $2 \times 2 \times 10 \text{ mm}^3$  LSO: Ce, Ca produced by Agile and one pair of  $6 \times 6 \times 3 \text{ mm}^3$  LYSO:Ce crystals from CPI [14] have also been measured for comparison and to provide a reference time detector for coincidence time resolution measurements.

The Garnet crystals were grown by Czochralski method at a speed of about 1 mm/hour and using an iridium crucible under  $N_2$ . For the GAGG samples, the seed crystal of  $\langle 100 \rangle$  orientation was purchased from C & A Corporation, Sendai, Japan. Mixtures of oxides of purity 5N with compositions of  $Gd_{2.982}Ce_{0.015}Ga_{2.7}Al_{2.3}O_{12}$  and  $Gd_{2.982}Ce_{0.015}Mg_{0.003}Ga_{2.7}Al_{2.3}O_{12}$  were used as starting materials. For the YAG and LuAG samples a stoichiometric mixture of 4N  $MgCO_3$ ,  $CeO_2$ ,  $a-Al_2O_3$ ,  $Y_2O_3$  and  $Lu_2O_3$  powders was used as starting material. Nominally, starting powders were prepared according to the formula of  $(Mg_{0.005}Ce_{0.0005}Lu_{0.99})_3Al_5O_{12}$  and  $(Mg_{0.005}Ce_{0.0005}Y_{0.99})_3Al_5O_{12}$  and seeds of  $\langle 111 \rangle$  oriented YAG crystals were used. All crystal were then cut to dimensions of  $2 \times 2 \times 10 \text{ mm}^3$  with the two end faces polished. The lateral faces were also polished for the reference samples and GAGG but not for the YAG and LuAG samples.

The scintillating properties of the samples, summarized in Table 1, were measured in laboratory using the same instrumentation and procedure described in [12]. The light yield was measured using a  $^{137}Cs$  source, wrapping the samples in several layers of Teflon and coupling them to a Hamamatsu Photonics R2059 photomultiplier tube (PMT) with optical grease (refractive index  $n=1.41$ ). The decay time measurements were performed using time correlated single photon counting [15], in which the start-detector is realized with a  $2 \times 2 \times 5 \text{ mm}^3$  LSO:Ce codoped 0.4% Ca scintillator coupled to a Hamamatsu S10931-050P SiPM and read out by the NINO chip [16]. The stop-detector was realized with a single photon avalanche diode of  $50 \mu\text{m}$  (ID-Quantique ID100-50) as discussed in [17]. A double-exponential fit was performed to estimate the decay time components according to the following parameterization,

$$A(t) = A_1 e^{-t/\tau_{d,1}} + A_2 e^{-t/\tau_{d,2}}$$

in which the relative intensity of the two components, in terms of total number of photons emitted, is given by

$$I_i = \frac{A_i \tau_{d,i}}{\sum A_i \tau_{d,i}}$$

The  $Mg^{2+}$ -codoped samples show a faster decay time due to the stabilization of the  $Ce^{4+}$  centres, which provide an alternative channel for fast radiative de-excitation and thus compete with any kind of electron traps in the material for the capture of an electron from the conduction band [12,18].

### 2.2. Experimental setup

The crystal samples were wrapped with several layers of Teflon as reflector and glued to a  $3 \times 3 \text{ mm}^2$  Hamamatsu S13360-3050PE SiPM using Meltmount glue with refractive index  $n=1.68$ . For the  $6 \times 6 \times 3 \text{ mm}^3$  LYSO:Ce crystals, larger area SiPMs were used (HPK  $6 \times 6 \text{ mm}^2$ ). The single cell size for both SiPMs is  $50 \mu\text{m}$ , the photon detection efficiency (PDE) has a maximum of 55% at 430 nm when operating bias voltage was set to about 9 V overvoltage ( $V_{br} \approx 52 \text{ V}$ ). The signal from the SiPM was read out using a customized board providing a fast time signal obtained with the NINO chip and the amplified analogue waveform as described in [22]. The signals were read out with a CAEN V1742 module, providing a fast digitization of up to 32 channels at 5 GS/s. Three NINO boards, instrumented with two SiPMs each, were used in parallel to allow the simultaneous measurement of 6 crystal samples as shown in Fig. 1. The boards were aligned with a mechanical support and placed inside a thermally isolated, light tight box with stable temperature of  $15 \pm 0.5 \text{ }^\circ\text{C}$ .

The same operating voltages for the NINO thresholds were applied to all the boards and the same bias voltage of 61.5 V was applied to power the  $3 \times 3 \text{ mm}^2$  HPK SiPMs (corresponding to about 9 V overvoltage). The larger  $6 \times 6 \text{ mm}^2$  HPK SiPMs used for the LYSO:Ce crystals were operating at 61 V (9 V over breakdown voltage).

A pion beam of 150 GeV momentum was provided by the H2 beam line at CERN which allows a precise selection of particles in the 10–250 GeV energy range by means of several magnets and collimator elements. High energy pions traversing a 10 mm long crystal have a small probability ( $\sim 3\%$ ) to interact via inelastic scattering and produce large energy deposits inside the crystal. In the majority of cases the pions will cross the whole crystal thickness depositing an energy close to the value of a minimum ionizing particle (mip), i.e. about  $k\rho \text{ MeV/cm}$  where  $\rho$  is the density of the compound (reported in Table 1) and  $k$  an empirical coefficient with values  $\sim 1.57$  for YAG and  $\sim 1.48$  for LuAG, GAGG and LSO. As a pion goes through the setup, it creates a signal in all the crystal samples aligned in the box. The time stamp of each channel is computed at the 50% of the corresponding NINO output

**Table 1**

Summary of crystal dimensions and density for the samples used in this study. Optical and scintillation parameters as measured in laboratory are also reported: decay time components ( $\tau_{d,i}$ ) with relative intensity ( $I_i$ ), light output measured using a PMT R2059 and  $^{137}Cs$  source. Values for reference crystals are also shown for comparison and were measured in [17]. The values of refractive index are taken from literature [19–21].

Dimensions [mm <sup>3</sup> ]	Crystal type	Density ( $\rho$ ) [g/cm <sup>3</sup> ]	Refractive index at 500 nm	$\tau_{d,1}$ [ns]	$I_1$ [%]	$\tau_{d,2}$ [ns]	$I_2$ [%]	LO [ph/MeV]
$2 \times 2 \times 10$	YAG:Ce	4.6	1.84	102	52	492	48	13000
$2 \times 2 \times 10$	YAG:Ce:Mg	4.6	1.84	59	84	225	16	17000
$2 \times 2 \times 10$	LuAG:Ce	6.7	1.86	98	33	1907	67	9000
$2 \times 2 \times 10$	LuAG:Ce:Mg	6.7	1.86	50	86	908	14	14000
$2 \times 2 \times 10$	GAGG:Ce	6.6	1.92	101	65	319	35	34700
$2 \times 2 \times 10$	GAGG:Ce:Mg	6.6	1.92	51	53	196	47	26700
$6 \times 6 \times 3$	LYSO:Ce	7.1	1.81	24	15	45	85	27000
$2 \times 2 \times 5$	LSO: Ce, Ca	7.4	1.81	8	6	33	94	22200

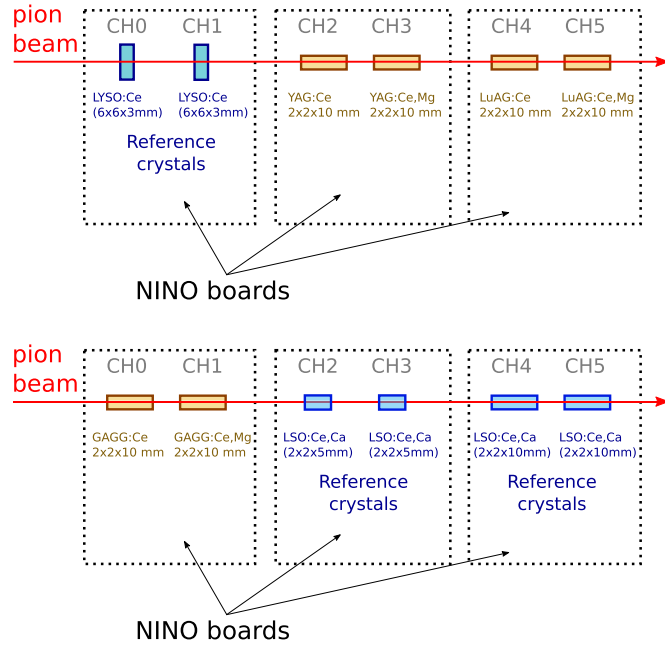


**Fig. 1.** Schematic representation of the experimental setup. Three NINO boards are used in parallel to allow simultaneous measurement of several samples. A pair of 3 mm thick LYSO:Ce crystals with section of  $6 \times 6 \text{ mm}^2$  were used as reference time detector during the first period of data taking whereas 5 and 10 mm thick LSO:Ce, Ca crystals with section  $2 \times 2 \text{ mm}^2$  were used for the second dataset.

amplitude and extracted from a linear fit of the signal leading edge. The maximum of the analogue waveform amplitude obtained from the SiPM analogue signal is then used to apply time walk corrections as discussed in [6].

A first set of data was taken using LYSO:Ce ( $6 \times 6 \times 3 \text{ mm}^3$ ) crystals as reference and measuring the YAG:Ce, YAG:Ce,Mg, LuAG:Ce and LuAG:Ce,Mg crystals. A second dataset consisted in two pairs of  $2 \times 2 \times 5 \text{ mm}^3$  and  $2 \times 2 \times 10 \text{ mm}^3$  LSO:Ce, Ca crystals used as reference, and one board instrumented with the GAGG:Ce and GAGG:Ce,Mg samples as shown in Fig. 1.

In order to select events in which the pion was traversing all crystals, a cut on the signal amplitude was made around the mip peak of each crystal. Fig. 2 shows the correlation plot for the signals detected in a pair of reference crystals and the corresponding amplitude cuts applied, represented by red lines. For all crystals the signal was clearly separated from the noise, the peak for the 3 mm thick crystals being broader due to larger Landau fluctuations. In addition, for each event a simultaneous mip-signal was required on all the other crystals in order to guarantee a straight trajectory of the beam particles.

As the coincidence time resolution in scintillating crystals is known to depend on the threshold value used to obtain the time stamp [3,23], a scan of the NINO threshold in the 50–2000 mV range has been done in order to evaluate the optimal operational value for each crystal +SiPM device.

### 3. Results

The time difference between a garnet crystal and a reference crystal (LYSO:Ce or LSO:Ce, Ca) has been calculated for each sample, with and without amplitude walk corrections. The coincidence time resolution (CTR) is then obtained with a Gaussian fit of the distributions as shown in Fig. 3 for reference samples and Fig. 5 for garnets. By comparing the coincidence time resolution of an identical pair of reference crystals+SiPMs (e.g. the LYSO:Ce or the LSO:Ce, Ca pairs shown in Fig. 3) it is possible to estimate the time resolution of the single reference detector as:

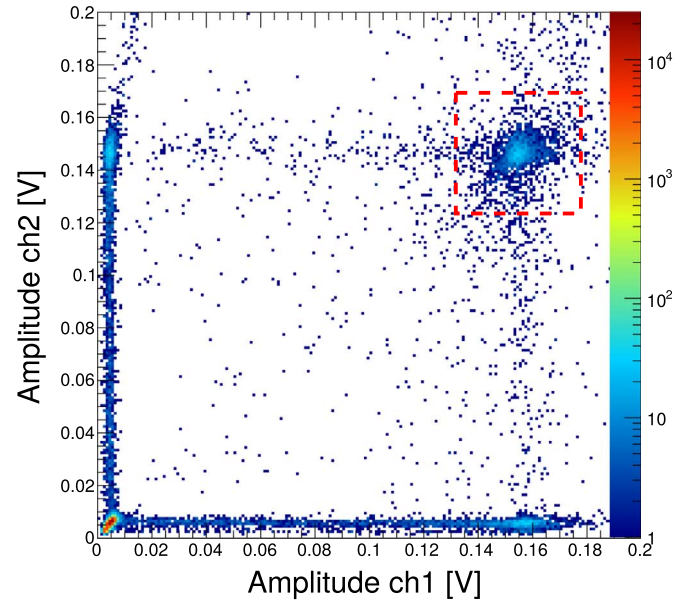
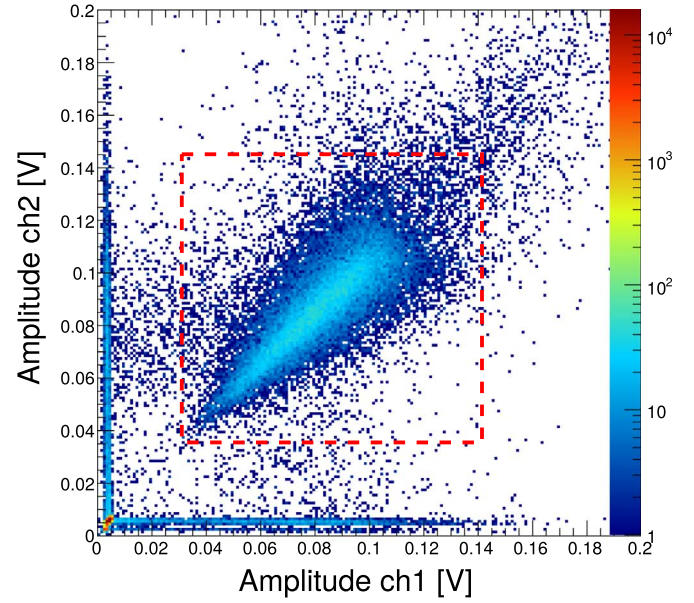


**Fig. 2.** Correlation of the signal amplitude and event selection applied (red lines) observed in two separate reference crystals for  $6 \times 6 \times 3 \text{ mm}^3$  LYSO:Ce crystals (top) and  $2 \times 2 \times 5 \text{ mm}^3$  LSO:Ce, Ca crystals (bottom).

$$\sigma_{i(\text{ref})} = \sigma_{CTR(\text{ref},\text{ref})} / \sqrt{2}$$

The timing performance of a single crystal+SiPM,  $\sigma_{i,i}$ , can then be obtained by comparison with a reference LYSO:Ce or LSO:Ce, Ca crystal by subtracting in quadrature the contribution of the reference crystal:

$$\sigma_{i,i} = \sqrt{\sigma_{CTR(i,\text{ref})}^2 - \sigma_{i(\text{ref})}^2}$$

This procedure is applied for each NINO threshold in the 50–2000 mV range and the results for single device time resolution,  $\sigma_t$ , are shown in Fig. 4 for the reference crystals and in Fig. 6 for the tested garnet samples. The time resolution shows a dependence on the applied threshold for all samples with some difference from crystal to crystal. At very low threshold values (below 150 mV), the CTR starts to deteriorate and can reach values as high as 100 ps for 50 mV. The optimal operation threshold is found to be around 1000 mV for the reference LYSO:Ce and LSO:Ce, Ca crystals, for which a single time resolution of about 17.5 ps is achieved. For YAG and LuAG samples we

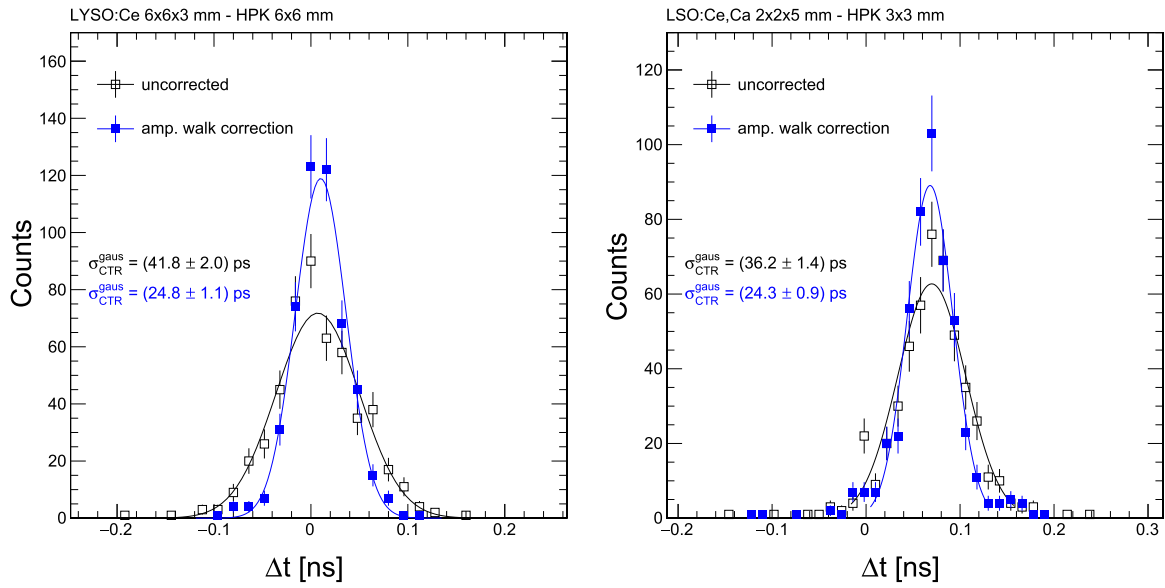


**Fig. 3.** Coincidence time resolution at the optimal NINO threshold (1000 mV) for the reference crystals: LYSO:Ce  $6 \times 6 \times 3$  mm<sup>3</sup> (left) and LSO:Ce, Ca  $2 \times 2 \times 5$  mm<sup>3</sup> (right).

observe a minimum of the time resolution value around 200 mV and a small degradation for higher thresholds, whereas for the GAGG samples the  $\sigma_t$  remains rather flat in the 500–2000 mV range. For the LuAG:Ce sample only the data at 1000 mV threshold are available due to an experimental malfunction of the setup occurred during the experiment. The peculiar shape of the  $\sigma_t$  vs NINO threshold for LuAG and YAG crystals can be attributed to the lower light yield of these samples with respect to GAGG and the reference crystals. Due to a poorer scintillation signal, the influence of prompt Cherenkov photons in such crystals (discussed in the next section) plays an enhanced role and is likely to be responsible for the observation of an optimal time resolution at low thresholds. The best time resolution obtained for each sample at its optimal NINO threshold is reported in Table 2 (Figs. 5 and 6).

All three types of aluminum garnet crystals show similar time resolution in the range of 36–43 ps which improves down to 23–30 ps for Mg-codoped samples. The exact values and uncertainty on these numbers are reported in Table 2. The error reported represents the statistical uncertainty in the Gaussian fit, limited by the poor statistics due to the small size of the sample with respect to the beam radius

**Table 2**

Summary of single device time resolution,  $\sigma_{t,corr.}^{single}$  for detection of 150 GeV pions, calculated at the optimal threshold for each crystal. The most probable (and mean) values of the energy deposited by a 150 GeV pion are also reported. In case of LuAG:Ce<sup>+</sup>, only the threshold of 1000 mV was available and is thus reported in this table although it is likely not the optimal value.

Dimensions [mm <sup>3</sup> ]	Crystal type	$E_{dep}^{peak}$ ( $E_{dep}^{mean}$ ) [MeV]	$\sigma_{t,corr.}^{single}$ [ps]
2×2×10	YAG:Ce	6.5 (7.2)	39.3 ± 2.0
2×2×10	YAG:Ce:Mg	6.5 (7.2)	24.9 ± 1.5
2×2×10	LuAG:Ce	8.8 (9.9)	43.2 ± 2.0*
2×2×10	LuAG:Ce:Mg	8.8 (9.9)	22.7 ± 1.5
2×2×10	GAGG:Ce	8.4 (9.8)	36.2 ± 2.0
2×2×10	GAGG:Ce:Mg	8.4 (9.8)	30.5 ± 1.4
6×6×3	LYSO:Ce	2.7 (3.2)	17.5 ± 1.1
2×2×5	LSO: Ce, Ca	4.7 (5.5)	17.2 ± 1.0

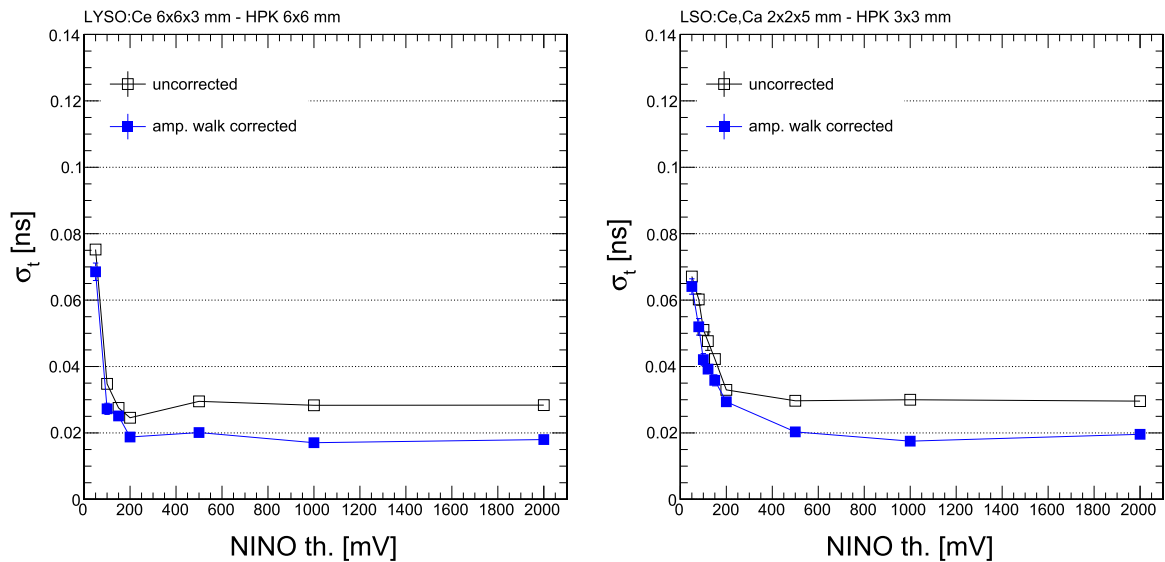


**Fig. 4.** Single device time resolution as a function of the NINO threshold for the reference crystals: LYSO:Ce  $6 \times 6 \times 3$  mm<sup>3</sup> (left) and LSO:Ce, Ca  $2 \times 2 \times 5$  mm<sup>3</sup> (right).

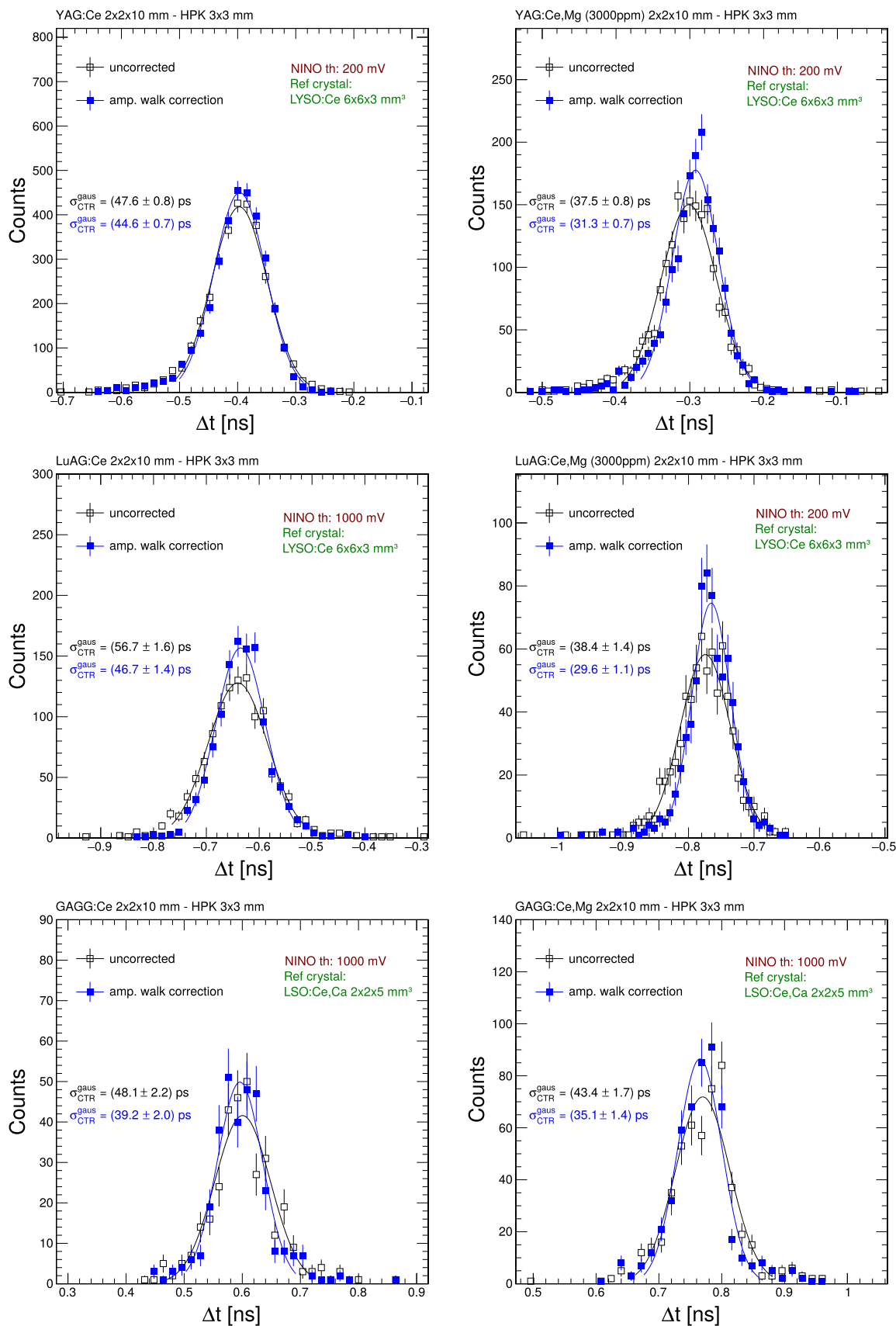


**Fig. 5.** Coincidence time resolution for the garnet crystals: YAG, LuAG and GAGG (at optimal NINO threshold), measured against the corresponding reference crystal (LYSO:Ce  $6 \times 6 \times 3 \text{ mm}^3$  for YAG and LuAG samples and LSO:Ce, Ca  $2 \times 2 \times 5 \text{ mm}^3$  for GAGG samples).

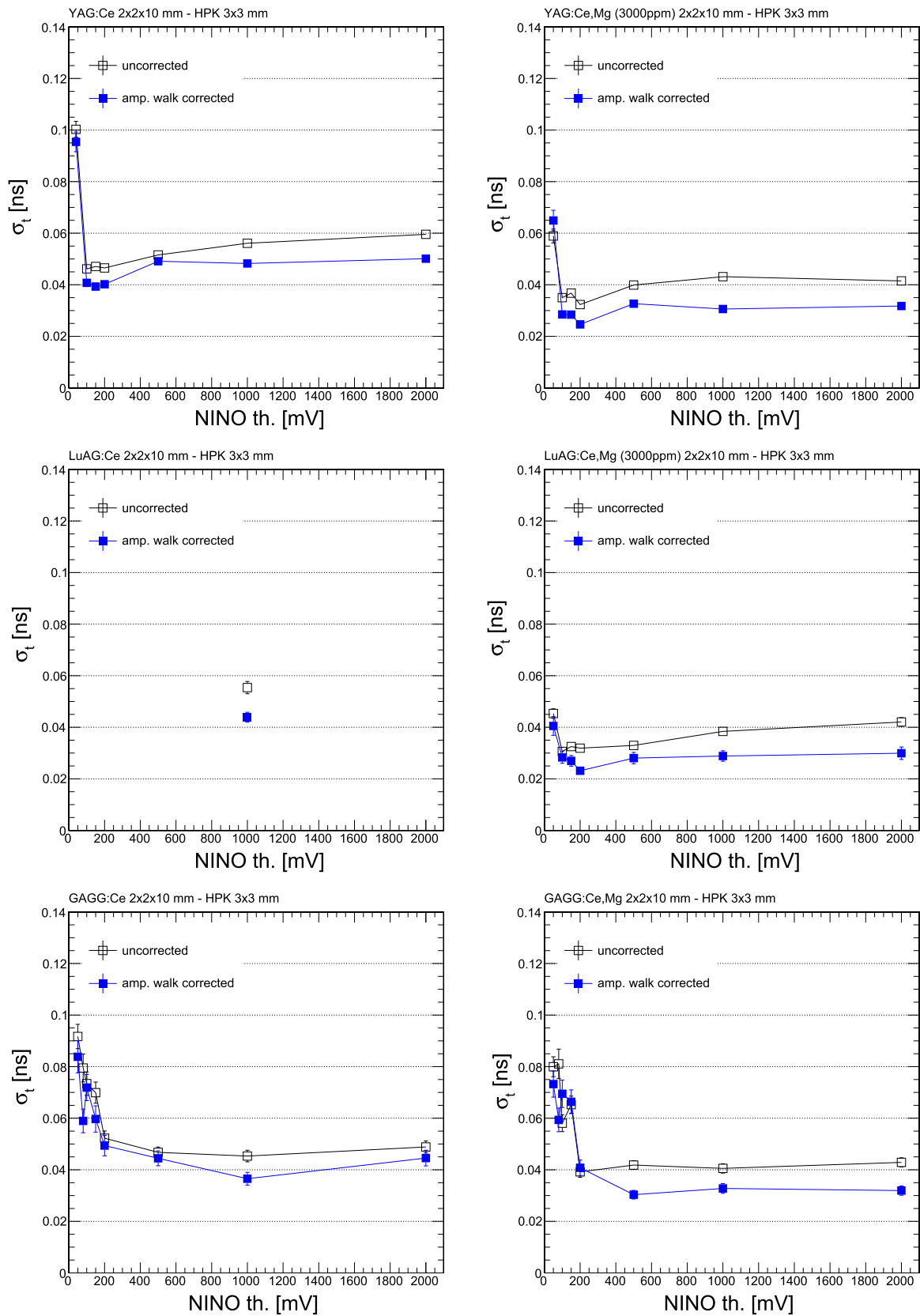


**Fig. 6.** Single device time resolution as a function of the NINO threshold for the garnet crystals: YAG, LuAG and GAGG (from top to bottom). For the LuAG:Ce crystal only value at 1000 mV is available as the corresponding channel was found to be malfunctioning during the acquisition of the other thresholds.

(about 1 cm). The value of time resolution observed for the LYSO:Ce crystal used as reference is compatible with previous measurement performed on similar samples with similar SiPMs (3x3 mm<sup>2</sup>

Hamamatsu TSV SiPM), yielding about 18 ps for 2 x 2 x 5 mm<sup>3</sup> LYSO:Ce crystals [6]. The present results also show that a thickness of 3 mm of LYSO:Ce can still provide an excellent time resolution

despite the smaller energy deposit of about 2.7 MeV. The single device time resolution of about 17 ps, achieved with  $2 \times 2 \times 5$  mm<sup>3</sup> LSO: Ce, Ca reference crystals, is worse than the value obtained in previous measurements with the same type of crystal but different SiPMs, which yielded about 10 ps. This difference can thus be attributed to the type of SiPMs used for the read-out. In the present test, Hamamatsu SiPMs with a protective epoxy window (refractive index  $n \sim 1.55$ ) were used. Conversely, for previous results, [6], a NUV-HD SiPM from FBK was used, with no protective window which allowed a better extraction of both scintillation and Cherenkov light.

#### 4. Discussion

The values of time resolution obtained for the aluminum garnet crystals clearly show that Mg-codoping is an effective way to improve the timing performance. This result can be understood in terms of the overall better scintillation properties of the codoped samples. Among the many parameters which characterize a scintillating crystal, the most relevant for timing applications are reported in Table 1. The intrinsic light yield of a sample is of great importance, however in this particular context where the interest is focused on the detection of minimum ionizing particles, the total light output is also affected by the density of the sample and its effective atomic number,  $Z$ , which determine the amount of average energy deposit per track length. Thus for a given crystal thickness, high  $Z$  and high density lead to a larger light output. A second fundamental parameter to determine the timing potential of a given scintillator is the kinetics of the scintillation pulse, i.e. the photon emission time distribution,  $f(t)$ , which can be described by the combination of exponential rise and decay time components ( $\tau_{r,i}$  and  $\tau_{d,i}$ ) according to the generic formula:

$$f(t) = \sum_i^N \frac{I_i}{\tau_{d,i} - \tau_{r,i}} \times [e^{-\frac{t}{\tau_{d,i}}} - e^{-\frac{t}{\tau_{r,i}}}] \quad (1)$$

where  $I_i$  is the relative intensity of a scintillation component  $i$ . The influence of these parameters has been widely discussed in [17,22] and predicts that, for a given light output ( $LO$ ), shorter decay times lead to better time resolution according to  $\sigma_t \propto \sqrt{\tau_d LO}$ . The wavelength of emitted light is also important since it should match the peak of the photon detection efficiency (PDE) of the SiPMs. For SiPMs used in this tests the PDE weighted for the scintillation emission is about 50% for LYSO:Ce and LSO: Ce, Ca crystals (emission peak around 420 nm), 45% for LuAG (emission peaks around 510 nm) and 43% for YAG and GAGG (emission peaks around 530 nm).

Cherenkov radiation is an additional source of photons, promptly produced at the passage of a charged particle and thus they can also improve the time resolution, especially in the test beam configuration due to the directionality of the Cherenkov light, whose emission angle describes a cone oriented towards the photodetector. The number of Cherenkov photons produced per track length,  $L$ , at a given wavelength,  $\lambda$ , depends mainly on the index of refraction of the material,  $n$ , according to:

$$\frac{d^2 N_{ph}}{dL d\lambda} = 2\pi\alpha z^2 \frac{1}{\lambda^2} \left(1 - \frac{1}{n^2}\right)$$

where  $\alpha = 1/137$  and  $z$  is the charge unit of the particle, and shows a  $1/\lambda^2$  dependence, i.e. more photons are emitted in the UV range.

The angular distribution of Cherenkov photons produced for different types of crystals is shown in Fig. 7 where the number of photons produced is reported as a function of the angle with respect to the crystal longitudinal axis,  $\theta$  (i.e. angle wrt the direction of the incoming pion). As expected, a sharp peak is present in correspondence of the Cherenkov cone, i.e.  $\approx \arccos(1/n)$ . Results are obtained using Geant4 ray tracing simulation software, where the refractive indices reported in Table 1 are used for the different type of crystals. As visible from Fig. 7, a low background of Cherenkov photons, isotropic with

respect to the pion direction of flight, is also produced by secondary charged particles emitted along the pion trajectory. Table 3 reports the angles corresponding to the Cherenkov cone for the crystal under study as well as the maximum angle of light extraction from the crystal end assuming an optical medium with refractive index 1.55 (e.g. the protective window in front of the SiPM). Thus, Table 3 shows how the high refractive index of GAGG: Ce, although responsible for a slightly larger number of Cherenkov photons produced ( $\sim 6\%$  more than in LSO: Ce), leads to a wider cone of emission which limits the probability to extract these photons because the extraction angle also becomes smaller with larger  $n$ . Assuming the beam is perfectly parallel to the crystal axis, i.e. perpendicular to the extraction face, Cherenkov photons would be extracted only for YAG and LSO samples which satisfy the condition  $\theta_c < \theta_{max}$ . Since in the experimental setup imperfect alignment can realistically lead to  $\sim 1^\circ$  angle between beam direction and crystal axis, a partial extraction of Cherenkov photons for LuAG crystals (about half of the Cherenkov cone) is likely to occur, although the beam-crystal misalignment is still insufficient for the extraction of Cherenkov photons in GAGG samples. The peculiar characteristics of our test beam setup can explain the slightly poorer performance of GAGG: Ce,Mg, despite its higher scintillation light yield, with respect to YAG: Ce,Mg and LuAG: Ce,Mg samples, as well as the difference in the value of the optimal NINO threshold. The production of Cherenkov light could be exploited also in GAGG crystals by tilting the setup of a few degrees ( $\sim 5^\circ$ ) with respect to the incoming particles. Another possibility to enhance light extraction would be to use optical couplants with index of refraction higher than  $n=1.55$ . The Meltmount glue used to couple the crystals to the SiPM has a refractive index of  $n=1.68$ , which allows the total extraction of Cherenkov photons also for GAGG. However, the photons are still reflected at the interface with the protective window of these particular SiPMs from HPK, having a refractive index around 1.55. For this reason, SiPMs without protective window, such as the FBK NUV-HD SiPM used in previous tests, [4,6,23], represent a viable strategy to further improve the timing performance of a crystal+SiPM detector.

From Fig. 7 and Table 3 it can be seen that about 640 Cherenkov photons are produced by a mip in 10 mm thick crystals in the wavelength range between 300 and 1200 nm. The total number of Cherenkov photons arriving at the photodetector is much smaller due to light self-absorption of the material at short wavelengths, imperfect surface state and the transmission cut-off of Meltmount glue ( $n=1.68$ ) at 400 nm. In Cerium activated Aluminum garnet crystals (YAG, LuAG, GAGG) the cutoff in light transmission spectra is around 500 nm whereas for L(Y)SO:Ce crystals it is around 400 nm. As a consequence, the wavelength distribution of detected Cherenkov photons peaks near the scintillation light emission maximum and has a long tail extending to the infra-red region. Taking into account these effects, we estimated a photon detection efficiency (PDE) for the Cherenkov photons arriving at the photodetector of 30% for LSO:Ce and 22% for the garnets (YAG: Ce, LuAG: Ce, GAGG: Ce). These considerations would lead to a number of detected Cherenkov photons of about 75 for the garnets and 100 for LSO:Ce assuming the angle of light extraction is large enough to avoid total internal reflection of Cherenkov light. These photons, originating along the pion track, would be distributed rather uniformly within a  $\sim 60$  ps time interval for LSO and  $\sim 70$  ps for GAGG, corresponding to the time required by the light to traverse the whole crystal length traveling at  $c/n$  and following the trajectory defined by the Cherenkov angle.

To better evaluate the influence of the Cherenkov component and study the effects discussed above, further tests are required where the angle between incident particle and crystal axis is varied. Similarly, a detailed comparison of the timing performance when the optical interface between crystal and SiPM is changed (e.g. using optical glue with higher refractive index, changing the refractive index of the SiPM protective window, etc...) can bring to further optimization of this technology.

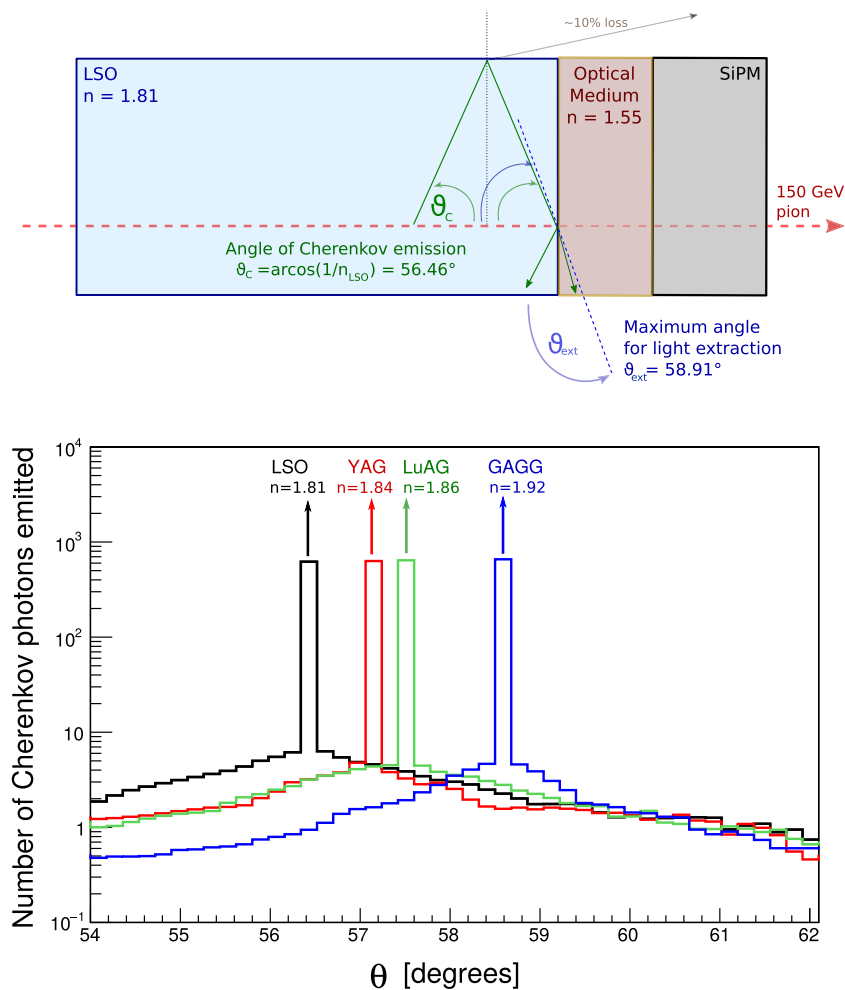


**Fig. 7.** Top: drawing of Cherenkov photon emission angle and maximum angle for light extraction for a LSO crystal. Bottom: number of Cherenkov photons produced in 10 mm thick LSO, YAG, LuAG and GAGG crystals (from left to right) as a function of the emission angle ( $\theta$ ).

**Table 3**

Refractive index,  $n$ , number of Cherenkov photons produced in a 10 mm long crystal within 300–1200 nm wavelength range,  $N_{ch}^{prod.}$ , emission angle of Cherenkov photons,  $\theta_c$ , and maximum angle for light extraction,  $\theta_{max}$ , for a given crystal assuming an optical interface with refractive index  $n=1.55$  at the extraction end.

Crystal type	$n$	$N_{ch}^{prod.}$	$\theta_c$	$\theta_{max}$
LSO	1.81	620	56.46	58.91
YAG	1.84	630	57.12	57.41
LuAG	1.86	640	57.50	56.48
GAGG	1.92	660	58.57	53.82

## 5. Conclusions

A comparison of the timing performance of different crystals read out with silicon photomultipliers has been carried out using 150 GeV pions from the CERN SPS facility. The results obtained on LYSO:Ce and LSO: Ce, Ca samples represent an extension and confirmation of previous tests, showing that a time resolution at the level of 17 ps can be achieved with a variety of crystal sizes and SiPMs from different manufacturers. A different family of inorganic scintillators, namely Lutetium-, Yttrium- and Gallium-Gadolinium- Aluminum Garnets doped with Cerium have been tested and demonstrated that when such crystals are codoped with  $Mg^{2+}$  ions a time resolution in the range of 23–30 ps is attainable. The present results confirm the potential of heavy scintillating crystals for precision timing applications. Their high scintillation light yield within a short decay time window are confirmed

to be crucial parameters to obtain an optimal time resolution. The radiation tolerance of these type of garnet crystals also makes them suitable candidates for applications in high radiation environments such as timing detectors at future colliders.

## Acknowledgments

This work was performed in the framework of the Crystal Clear Collaboration and received funding from the European Union's Horizon 2020 research and innovation program under the Marie Skłodowska-Curie grant agreement no. 644260 (Intelum) and from the ERC Advanced grant no. 338953 (TICAL). Support has been received also from ASCIMAT project under grant agreement no. 690599 and from COST Action TD1401 (FAST). We also acknowledge the support received by the Czech Science Foundation 16-15569S and from the CERN SPS facility experts and CMS colleagues which made these measurements possible.

## References

- [1] W.W. Moses, et al., Time of flight in PET revisited, IEEE Trans. Nucl. Sci. 50 (2003) 1325–1330. <http://dx.doi.org/10.1109/TNS.2003.817319>.
- [2] M. Conti, et al., State of the art and challenges of time-of-flight PET, Phys. Med. 25 (2009) 1. <http://dx.doi.org/10.1016/j.ejmp.2008.10.001>.
- [3] S. Gundacker, et al., Time resolution deterioration with increasing crystal length in a TOF-PET system, Nucl. Instrum. Methods Phys. Res. A 737 (2014) 92–100. <http://dx.doi.org/10.1016/j.nima.2013.11.025>.
- [4] S. Gundacker, et al., State of the art timing in TOF-PET detectors with LuAG, GAGG and L(Y)SO scintillators of various sizes coupled to FBK-SiPMs, J. Instrum. 11 (08)

- (2016) P08008 (URL (<http://stacks.iop.org/1748-0221/11/i=08/a=P08008>)).
- [5] CMS Collaboration, Technical proposal for the Phase-II upgrade of the Compact Muon Solenoid, CERN-LHCC-2015-010 (2015) LHCC–P–008.
- [6] A. Benaglia, S. Gundacker, P. Lecoq, M.T. Lucchini, A. Para, K. Pauwels, E. Auffray, Detection of high energy muons with sub-20 ps timing resolution using L(Y)SO crystals and SiPM readout, Nucl. Instrum. Meth A830 (2016) 30–35. <http://dx.doi.org/10.1016/j.nima.2016.05.030>.
- [7] M.A. Spurrier, et al., Effects of  $\text{Ca}^{2+}$  co-doping on the scintillation properties of LSO:Ce, IEEE Trans. Nucl. Sci. 55 (2008) 1178–1182. <http://dx.doi.org/10.1109/TNS.2007.913486>.
- [8] S. Blahuta, et al., Evidence and consequences of  $\text{Ce}^{++}$  in LYSO: ce,ca and LYSO:Ce,Mg single crystals for medical imaging applications, IEEE Trans. Nucl. Sci. 60 (2013) 3134–3141. <http://dx.doi.org/10.1088/0031-9155/60/12/4635>.
- [9] M. Nikl, et al., Defect engineering in Ce-doped aluminum garnet single crystal scintillators, Cryst. Growth Des. 14 (2014) 4827–4833. <http://dx.doi.org/10.1021/cg501005s>.
- [10] A. Nagura, et al., Improvement of scintillation properties on Ce doped  $\text{Y}_3\text{Al}_5\text{O}_{12}$  scintillator by divalent cations co-doping, Jpn. J. Appl. Phys. 54 (2015) 04DH17. <http://dx.doi.org/10.7567/JJAP.54.04DH17>.
- [11] A. Petrosyan, et al., A study of radiation effects on LuAG: Ce(Pr) co-activated with Ca, J. Cryst. Growth 430 (2015) 46–51. <http://dx.doi.org/10.1016/j.jcrysgro.2015.08.019>.
- [12] M. Lucchini, V. Babin, P. Bohacek, S. Gundacker, K. Kamada, M. Nikl, A. Petrosyan, A. Yoshikawa, E. Auffray, Effect of  $\text{Mg}^{2+}$  ions co-doping on timing performance and radiation tolerance of Cerium doped  $\text{Gd}_3\text{Al}_2\text{Ga}_3\text{O}_{12}$  crystals, Nucl. Instrum. Meth A816 (2016) 176–183. <http://dx.doi.org/10.1016/j.nima.2016.02.004> (<http://www.sciencedirect.com/science/article/pii/S0168900216001480>).
- [13] M.T. Lucchini, et al., Radiation tolerance of LuAG:Ce and YAG:Ce crystals under high levels of gamma- and proton-irradiation, IEEE Trans. Nucl. Sci. 99 (2016). <http://dx.doi.org/10.1109/TNS.2015.2493347> accepted for publication.
- [14] T. Kimble, M. Chou, B. Chai, Scintillation properties of lyso crystals, IEEE Nuclear Science Symposium and Medical Imaging Conference, 3, 2002, pp. 1434–1437. (<https://www.scopus.com/inward/record.uri?Eid=2-s2.0-0142210131&partnerID=40&md5=6e17532447b761301f0e51fe216a04da>)
- [15] L.M. Bollinger, et al., Measurement of the time dependence of scintillation intensity by a delayed coincidence method, Rev. Scientif. Instrum. 32 (1961) 1044. <http://dx.doi.org/10.1063/1.1717610>.
- [16] S. Gundacker et al., SiPM photodetectors for highest time resolution in PET, Proceedings of Science PoS(PhotoDet 2012)016. LAL Orsay.
- [17] S. Gundacker et al., Measurement of intrinsic rise times for various L(Y)SO and LuAG scintillators with a general study of prompt photons to achieve 10 ps in TOF-PET, Phys. Med. Biol. (2015) accepted for publication.
- [18] Y. Wu, et al., Role of  $\text{Ce}^{4+}$  in the scintillation mechanism of co-doped  $\text{Gd}_3\text{Al}_2\text{Ga}_3\text{O}_{12}:\text{Ce}$ , Phys. Rev. Appl. 2 (41) (2014) 044009. <http://dx.doi.org/10.1103/PhysRevApplied.2.044009>.
- [19] N.S. Kozlova, et al., Optical properties and refractive indices of  $\text{Gd}_3\text{Al}_2\text{Ga}_3\text{O}_{12}^{3+}$  crystals, Crystallogr. Rep. 61 (3) (2016) 474–478. <http://dx.doi.org/10.1134/S1063774516030160> (<http://dx.doi.org/10.1134/S1063774516030160>).
- [20] G. Jellison et al., Spectroscopic refractive indices of monoclinic single crystal and ceramic lutetium oxyorthosilicate from 200 to 850 nm, Journal of Applied Physics, 112 (6). (<http://scitation.aip.org/content/aip/journal/jap/112/6/10.1063/1.4752421>)<http://dx.doi.org/10.1063/1.4752421>
- [21] Y. Kuwano, et al., Crystal growth and properties of  $(\text{Lu},\text{Y})_3\text{Al}_5\text{O}_{12}$ , J. Cryst. Growth 260 (1–2) (2004) 159–165. <http://dx.doi.org/10.1016/j.jcrysgro.2003.08.060> (<http://www.sciencedirect.com/science/article/pii/S0022024803016749>).
- [22] S. Gundacker, et al., Time of flight positron emission tomography towards 100 ps resolution with L(Y)SO an experimental and theoretical analysis, JINST 8 (2013) P07014. <http://dx.doi.org/10.1088/1748-0221/8/07/P07014>.
- [23] M. Nemallapudi, et al., Sub-100 ps coincidence time resolution for positron emission tomography with LSO:Ce codoped with Ca, Phys. Med. Biol. 60 (2015) 4635–4649. <http://dx.doi.org/10.1088/0031-9155/60/12/4635>.